

Time-resolved dynamics of resonant and nonresonant broadband picosecond coherent anti-Stokes Raman scattering signals

Sukesh Roy^{a)} and Terrence R. Meyer

Innovative Scientific Solutions, Inc., 2766 Indian Ripple Road, Dayton, Ohio 45440

James R. Gord

Air Force Research Laboratory, Propulsion Directorate, Wright-Patterson AFB, Ohio 45433

(Received 3 August 2005; accepted 29 November 2005; published online 28 December 2005)

The time-resolved dynamics of resonant and nonresonant broadband picosecond coherent anti-Stokes Raman scattering (CARS) signals in gas-phase media are investigated. For ~ 135 ps pump and probe beams and ~ 106 ps Stokes beams, the magnitude of the nonresonant signals are decreased by more than three orders of magnitude when the probe beam is delayed by ~ 110 ps, whereas the resonant nitrogen CARS signal is reduced only by a factor of 3. Investigation of these time dynamics is important for understanding the optimal time delay for nonresonant background suppression as well as for understanding the collisional and Doppler dependence of the resonant CARS signals. © 2005 American Institute of Physics. [DOI: 10.1063/1.2159576]

Coherent anti-Stokes Raman scattering (CARS) spectroscopy of nitrogen is widely used for temperature measurements in reacting flows and plasmas.^{1,2} In air-breathing combustion environments, measurements of temperature using nitrogen CARS have the advantage that nitrogen is present at high concentrations almost everywhere in the combustor. Most previous CARS thermometric measurements in gas phase or reacting flows have been performed using nanosecond laser pulses. A major limitation of nanosecond-laser-based CARS thermometry is the contribution of the nonresonant signal, which limits the accuracy and degrades the sensitivity of the technique.³ The nonresonant background can be suppressed by polarization selection, but this results in a reduction of the resonant CARS signal by at least a factor of sixteen.³

There have been relatively few demonstrations of picosecond CARS in the gas phase, and all previous measurements in both liquids and gases have been performed using synchronously pumped dye lasers, which do not allow the acquisition of single-shot spectra for unsteady flows.⁴⁻⁷ In unsteady flows, where there is significant variation in temperature and density, measurement of the CARS signal using a tunable source such as a synchronously pumped dye laser, optical parametric amplifier, or distributed-feedback dye laser leads to a distortion of the spectra biased toward low temperatures. This is due to the requirement of scanning the dye lasers or the OPA for the acquisition of spectrum covering a bandwidth of ~ 20 – 100 cm^{-1} , especially at temperatures relevant to combustion. We have recently demonstrated picosecond CARS measurements using a broadband modeless dye laser with sufficient bandwidth to excite the full ro-vibrational transition band in a single shot,⁸ thereby enabling nonresonant background suppression while avoiding temperature bias in unsteady flows.

Recently, CARS thermometry using femtosecond laser pulses has also been demonstrated.⁹ Both picosecond and femtosecond CARS systems permit nonresonant background suppression and enable the investigation of molecular-

ensemble collisional dynamics. Relatively straightforward substitution of picosecond lasers into well-established broadband nanosecond CARS systems will enable single-shot thermometry in practical combustion environments; however, femtosecond CARS thermometry will require considerable further development to achieve such measurements.¹⁰

The objective of this work is to investigate the time-resolved dynamics of the broadband picosecond resonant pure-nitrogen CARS signal along with the nonresonant signals from argon, oxygen, and carbon dioxide. This will provide an understanding of the time frame required for effective suppression of the nonresonant contribution to the CARS signal as well as an understanding of the nitrogen-nitrogen collisional-Doppler dephasing and relaxation processes in the ensemble. The dependence of the broadband picosecond CARS signal on pressure and temperature is the subject of ongoing research and will be addressed in a companion letter. The current study is focused on determining the appropriate delay time for the probe beam with respect to the pump beam so as to suppress the nonresonant contribution to the resonant CARS signal. In the liquid phase, time-resolved observation of the resonant and nonresonant contribution to the third-order nonlinear susceptibility using picosecond CARS has been studied by Zinth *et al.*⁶ As expected, the authors observed a distinct temporal behavior for the resonant and nonresonant signals.

The laser wavelengths in the current experiment are selected to excite the rovibrational transition manifold of the nitrogen molecule while being nonresonant to argon, oxygen, and carbon dioxide. The nearly transform-limited frequency-doubled ~ 135 ps output of a Nd:YAG regenerative amplifier at 532 nm is used for the pump and probe beams, and the ~ 106 ps output of a broadband modeless dye laser at 606 nm is used as the Stokes beam. The temporal pulsewidths of the laser beams, measured with a Hamamatsu streak camera (Model C5680-21/M5676), are shown in Fig. 1. Each profile is averaged over ten laser shots. The solid lines shown in Fig. 1 are Gaussian envelopes fitted through the data points and are shown to indicate the deviation of the laser pulsewidths from Gaussian profiles. Further details on

^{a)} Author to whom correspondence should be addressed; electronic mail: sroy@woh.rr.com

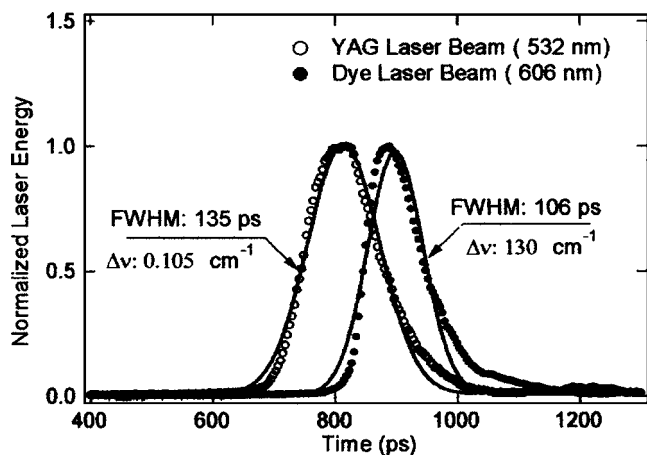


FIG. 1. Temporal profiles of the Nd:YAG and dye-laser beams acquired with a Hamamatsu streak camera. The solid lines are Gaussian profiles fitted through the data points. The profiles are shifted temporally for clarity.

the design and performance of the broadband picosecond CARS system are described elsewhere.⁸

For these experiments, a CARS polarization is induced in the medium by the narrowband pump and the broadband Stokes beams by overlapping them both spatially and temporally. A variable-delay probe beam is then used to investigate the induced polarization. The energy level diagram of the resonant and nonresonant contributions to the CARS signal is shown in Fig. 2.^{1,4} The nonresonant signal appears as a broad background that interferes with and distorts the CARS spectrum. The contribution from the nonresonant background is highest when all the laser beams are overlapped temporally and can significantly affect temperature accuracy, especially in hydrocarbon-rich environments due to the high nonresonant susceptibility of hydrocarbon compounds.

A typical room-temperature CARS spectrum in pure nitrogen and a nonresonant spectrum in pure argon averaged over 100 laser shots are shown in Fig. 3; these spectra are acquired with all laser beams arriving at the probe volume

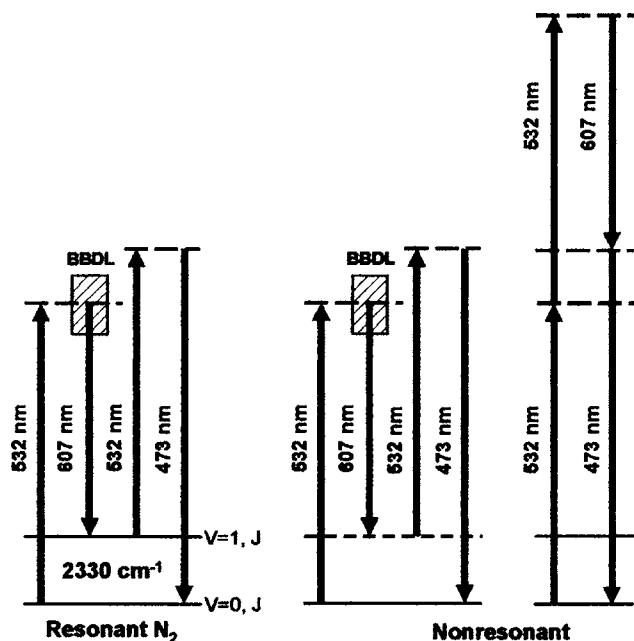


FIG. 2. Energy-level diagrams of the resonant and nonresonant processes that contribute to the CARS signal.

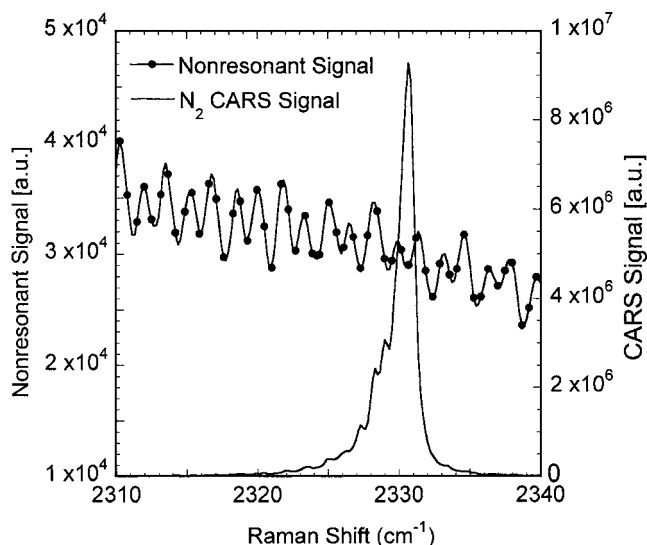


FIG. 3. A typical room temperature CARS spectrum in pure nitrogen and a pure nonresonant spectrum in argon averaged over 100 laser shots.

simultaneously. The nitrogen spectrum represents the overlapping *Q*-branch transition in the $v=0 \rightarrow v=1$ band in the ground electronic level. Modulation in the nonresonant spectrum is due to etalon effects from the dye cells of the modeless dye laser. The time-resolved resonant CARS signal in pure nitrogen and the nonresonant signal acquired by flowing pure argon, oxygen, and carbon dioxide are shown in Fig. 4 as a function of the time delay between the pump and probe beams. Each data point represents the integrated signal over an entire spectrum, such as that shown in Fig. 3, for a fixed time delay between the pump and probe beams. From Fig. 4, it is evident that the magnitudes of all the nonresonant signals are decreased by more than three orders of magnitude when the probe beam is delayed by ~ 110 ps with respect to the pump beam. Note that the full width half maximum temporal envelope of the Stokes beam is ~ 106 ps while that of the pump or probe beam is ~ 135 ps, as shown in Fig. 1. The magnitude of the resonant CARS signal is highest when the beams are overlapped temporally due to the nonresonant contribution to the resonant CARS signal. The signal decays as the probe beam is delayed with respect to the pump beam due to dephasing of the pump/Stokes-induced polarization. At approximately 130 ps, the slope of decline in the signal

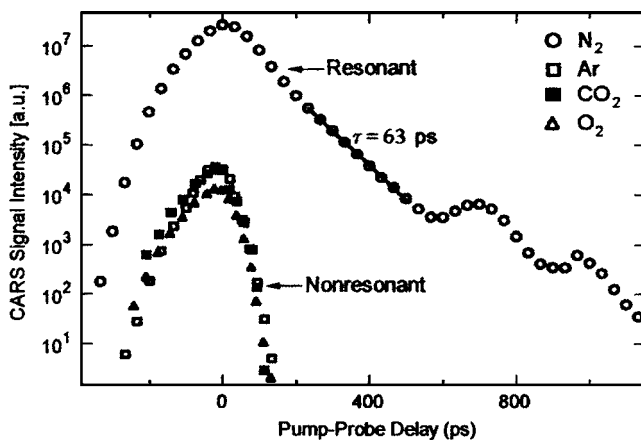


FIG. 4. Time-resolved resonant and nonresonant signals as functions of pump-probe time delay displaying the behavior of the resonant and nonresonant CARS signal.

changes, indicating the disappearance of the nonresonant contribution to the CARS signal.

The data in Fig. 4 indicate the magnitude of the CARS signal is reduced by a factor of 3 while the nonresonant signal is reduced by over three orders of magnitude at ~ 110 ps. Beyond 130 ps, the signal decays exponentially with $\tau=63$ ps due to collision-induced dephasing and rotational energy transfer.¹¹ The oscillation of the signal after ~ 500 ps is due to the constructive and destructive interference between the CARS signal generated from different rovibrational transitions excited by the broadband CARS system dictated by the phase differences between them.

In summary, we demonstrate that the broadband picosecond CARS system described here can be used to suppress the nonresonant contribution preferentially while enabling single-shot measurements typical of broadband nanosecond-laser-based systems. In future work, the time-resolved study described here will be extended to include the effects of Doppler and collisional broadening for a wide range of temperatures and pressures.

Funding for this research was provided by the Air Force Research Laboratory, Propulsion Directorate, Wright-Patterson AFB, under Contract No. F33615-03-D-2329-DO 002, and by the Air Force Office of Scientific Research (Anne Mutsuura, Program Manager).

¹A. C. Eckbreth, *Laser Diagnostics for Combustion Temperature and Species*, 2nd ed. (Gordon and Breach, St. Leonards, Australia, 1996).

²K. Kohse-Hoinghaus and J. B. Jeffries, *Applied Combustion Diagnostics* (Taylor and Francis, New York, 2002).

³A. C. Eckbreth and R. J. Hall, *Combust. Sci. Technol.* **55**, 175 (1981).

⁴F. M. Kanga and M. G. Sceats, *Opt. Lett.* **5**, 126 (1980).

⁵V. Mozorov, S. Mochalov, A. Olenin, V. Tunkin, and A. Kouzov, *J. Raman Spectrosc.* **34**, 983 (2003).

⁶W. Zinth, A. Laubereau, and W. Kaiser, *Opt. Commun.* **26**, 457 (1978).

⁷H. Graener, A. Laubereau, and J. W. Nibler, *Opt. Lett.* **9**, 165 (1984).

⁸S. Roy, T. R. Meyer, and J. R. Gord, *Opt. Lett.* **30**, 3222 (2005).

⁹P. Beaud, H. M. Frey, T. Lang, and M. Motzkus, *Chem. Phys. Lett.* **344**, 407 (2001).

¹⁰T. Long and M. Motzkus, *J. Opt. Soc. Am. B* **19**, 340 (2002).

¹¹G. Knopp, P. Beaud, P. Radi, M. Tulej, B. Bougie, D. Cannavo, and T. Gerber, *J. Raman Spectrosc.* **33**, 861 (2002).